ARTICLES
PUBLISHED ONLINE: 28 NOVEMBER 2010 | DOI: 10.1038/NCHEM.905
nature chemistry

Highly efficient photocatalytic oxygenation reactions using water as an oxygen source

Shunichi Fukuzumi[1,2]*, Takashi Kishi[1], Hiroaki Kotani[1], Yong-Min Lee[2,3] and Wonwoo Nam[2,3]*

The effective utilization of solar energy requires photocatalytic reactions with high quantum efficiency. Water is the most abundant reactant that can be used as an oxygen source in efficient photocatalytic reactions, just as nature uses water in an oxygenic photosynthesis. We report that photocatalytic oxygenation of organic substrates such as sodium *p*-styrene sulfonate occurs with nearly 100% quantum efficiency using manganese(III) porphyrins as an oxygenation catalyst, $[Ru^{II}(bpy)_3]^{2+}$ (bpy = 2,2′-bipyridine) as a photosensitized electron-transfer catalyst, $[Co^{III}(NH_3)_5Cl]^{2+}$ as a low-cost and weak one-electron oxidant, and water as an oxygen source in a phosphate buffer solution (pH 7.4). A high-valent manganese-oxo porphyrin is proposed as an active oxidant that effects the oxygenation reactions.

Oxygenic photosynthesis uses water, in its abundance, as a reactant to convert solar energy into chemical energy[1–6]. In this process, molecular oxygen is formed, to be used in various enzymatic reactions. For example, cytochrome P450 catalyses a number of important metabolic oxidation reactions by activating dioxygen[7,8]. The remarkable activities of these enzymes are ascribed to the formation of iron(IV)–oxo porphyrin π-radical cations, the so-called Compound I (Cpd I), as active oxidants in the enzymatic reactions. The stoichiometry of the catalytic oxygenation of organic substrates (RH) by O_2 requires reductive activation of dioxygen using two electrons and two protons[7–10]:

$$RH + O_2 + 2e^- + 2H^+ \rightarrow ROH + H_2O \quad (1)$$

In such a case, O_2 can be replaced by H_2O_2. Indeed, the formation of an iron(IV)–oxo porphyrin π-radical cation was observed in the reaction of horseradish peroxidase (HRP) and H_2O_2 (refs 9,10).

The use of synthetic metalloporphyrins has provided valuable mechanistic insight into the molecular catalytic mechanism of P450 (refs 11–15). Groves and colleagues reported P450-type activity in a model system using iron(III) porphyrins $[(Por)Fe^{III}(Cl)]$ and artificial oxidants, in which iron(IV)–oxo porphyrin π-radical cations were formed in a so-called 'shunt' pathway[14,15]. Since then, various metalloporphyrins, including manganese(III) porphyrins, have been used as catalysts in biomimetic oxygenation reactions[13–21].

The same oxidation state as H_2O_2 would be obtained by the two-electron oxidation of H_2O. In such a case, the stoichiometry of catalytic oxygenation of RH by H_2O requires oxidative activation of H_2O, in which two electrons and two protons should be removed as in equation (2):

$$RH + H_2O - 2e^- - 2H^+ \xrightarrow{\text{catalyst}} ROH \quad (2)$$

Although such oxidative activation of H_2O for the catalytic oxygenation of substrates requires strong one-electron oxidants (for example, cerium(IV) ammonium nitrate)[22,23], the strong one-electron oxidants could be replaced by much weaker oxidants, provided that the reaction is light-driven. Gray and colleagues indeed reported that Cpd I was produced in the photocatalytic oxidation of HRP (refs 24,25). However, there has been no report of the photocatalytic oxidative activation of water in oxygenation reactions using water as an oxygen source.

We report highly efficient photocatalytic olefin epoxidation, alkane hydroxylation and sulfoxidation reactions by using manganese porphyrins as a catalyst, $[Ru^{II}(bpy)_3]^{2+}$ (bpy = 2,2′-bipyridine) as a photosensitizer, $[Co^{III}(NH_3)_5Cl]^{2+}$ as a low-cost and weak one-electron oxidant[24,25], and water as an oxygen source. The photoinduced electron-transfer oxidation of manganese porphyrins by $[Co^{III}(NH_3)_5Cl]^{2+}$ is efficiently mediated by $[Ru^{II}(bpy)_3]^{2+}$ in a phosphate buffer solution (pH 7.4), and the photodynamics is studied by laser flash photolysis measurements to clarify the photocatalytic mechanism. It should be noted that cobalt ions used as oxidants in this study are earth-abundant materials, and have recently been used as effective catalysts for electrochemical water oxidation[26].

Results and discussion

Photoirradiation ($\lambda > 430$ nm) of a phosphate buffer solution (pH 7.4) containing sodium *p*-styrene sulfonate (NaSS), a manganese porphyrin catalyst [(TMPS)Mn^{III}(OH) or (TDCPS)Mn^{III}(OH)] (see footnote in Table 1), $[Ru^{II}(bpy)_3]^{2+}$ and $[Co^{III}(NH_3)_5Cl]^{2+}$ afforded *p*-styrene epoxide sulfonate as a major product with a yield of >90% based on the amount of $[Co^{III}(NH_3)_5Cl]^{2+}$ used as a one-electron oxidant (Table 1). The incorporation of an O atom from water into the oxygenated product was confirmed by carrying out the epoxidation of styrene in a phosphate buffer solution prepared with $H_2^{18}O$ (Supplementary Fig. S1). Similarly, the photocatalytic hydroxylation of sodium 4-ethylbenzene sulfonate (NaES) and oxygenation of 2-(methylthio)ethanol (MeSEtOH) produced the corresponding secondary alcohol and sulfoxide, with a high turnover number, respectively (Table 1). When $[Co^{III}(NH_3)_5Cl]^{2+}$ was replaced by other one-electron oxidants (such as $[Ru^{III}(NH_3)_6]^{3+}$), no photocatalytic epoxidation of NaSS and hydroxylation of NaES occurred under identical reaction conditions, indicating that the choice of an appropriate oxidant is essential. Of course, the photocatalytic oxygen-

[1]Department of Material and Life Science, Division of Advanced Science and Biotechnology, Graduate School of Engineering, Osaka University, SORST, Japan Science and Technology Agency (JST), Suita, Osaka 565-0871, Japan, [2]Department of Bioinspired Science, Ewha Womans University, Seoul 120-750, Korea, [3]Department of Chemistry and Nano Science, Center for Biomimetic Systems, Ewha Womans University, Seoul 120-750, Korea.
*e-mail: fukuzumi@chem.eng.osaka-u.ac.jp; wwnam@ewha.ac.kr

Table 1 | Turnover numbers (TON) for the photocatalytic oxygenation of NaSS, NaES and MeSEtOH by (Por)Mn^{III}(OH) and [Ru^{II}(bpy)$_3$]$^{2+}$ in the presence of [Co^{III}(NH$_3$)$_5$Cl]$^{2+}$ in phosphate buffered D$_2$O (pH 7.4).

Catalyst*	Substrate	Product	TON†	Yield (%)‡
(TMPS)Mn^{III}(OH)	NaSS	Epoxide	450	45
(TDCPS)Mn^{III}(OH)	NaSS	Epoxide	460	46
(TMPS)Mn^{III}(OH)	NaES	Alcohol	60	6
(TDCPS)Mn^{III}(OH)	NaES	Alcohol	70	7
(TMPS)Mn^{III}(OH)	MeSEtOH	Sulfoxide	30	3

Reaction conditions: (Por)Mn^{III}(OH) (1.0×10^{-5} M), [Ru^{II}(bpy)$_3$]$^{2+}$ (1.0×10^{-4} M), substrate (1.0×10^{-2} M), [Co^{III}(NH$_3$)$_5$Cl]$^{2+}$ (1.0×10^{-2} M). Photoirradiation with a Xe lamp through a cut filter ($\lambda > 430$ nm) for 15 min. *TMPS and TDCPS: 5,10,15,20-tetrakis(2,4,6-trimethyl-3-sulfonatophenyl)porphyrin and 5,10,15,20-tetrakis(2,6-dichloro-3-sulfonatophenyl)porphyrin, respectively. †TON is calculated from (mol of product)/(mol of catalyst). ‡Yield (%) is calculated from (mol of product)/(mol of initial substrate) ×100. Note that the maximum yield is 50% because the product yield is one-half of the conversion of the oxidant.

ation reactions did not yield products in the absence of the manganese porphyrin catalyst or the [Ru^{II}(bpy)$_3$]$^{2+}$ photosensitizer.

The quantum yields (Φ) of the photocatalytic epoxidation of NaSS were determined using a ferrioxalate actinometer (see Supplementary Information) under irradiation with monochromatic light ($\lambda = 450$ nm). The Φ value for the full solar spectrum should be smaller than that for visible wavelengths, because Ru(II) can absorb only in the 400–500 nm region. It should be noted that there is no dependence of an excitation wavelength at 400–500 nm. The Φ value increases with increasing [Co^{III}(NH$_3$)$_5$Cl]$^{2+}$ concentration, to reach a constant value close to 50% (Fig. 1a). This is nearly the 100% quantum efficiency expected from the stoichiometry of the photocatalytic oxygenation, because two photons are required for the two-electron oxidation of the substrate to produce one molecule of epoxide.

The Φ value also increases with increasing NaSS concentration to reach a constant value (Fig. 1b). The photocatalytic oxygenation of NaSS with [Co^{III}(NH$_3$)$_5$Cl]$^{2+}$ may start by photoinduced electron transfer from [Ru^{II}(bpy)$_3$]$^{2+\star}$ (where $\star$ denotes the excited state) to [Co^{III}(NH$_3$)$_5$Cl]$^{2+}$ (Fig. 2). In this case, the emission of [Ru^{II}(bpy)$_3$]$^{2+\star}$ is quenched by [Co^{III}(NH$_3$)$_5$Cl]$^{2+}$ (Supplementary Fig. S2). The quenching constant is determined from the slope of the Stern–Volmer plot as $K_q = 500\ M^{-1}$, which agrees with the reported value[27]. If the photocatalytic oxygenation of NaSS with [Co^{III}(NH$_3$)$_5$Cl]$^{2+}$ occurs with 100% efficiency after generation of [Ru^{III}(bpy)$_3$]$^{3+}$, the observed dependence of Φ on the concentration of [Co^{III}(NH$_3$)$_5$Cl]$^{2+}$ would be given by

$$\Phi = 0.5K_q[[Co^{III}(NH_3)_5Cl]^{2+}]/(1 + K_q[[Co^{III}(NH_3)_5Cl]^{2+}]) \quad (3)$$

The solid line in Fig. 1a is constructed according to equation (3), using the K_q value ($500\ M^{-1}$) determined by the emission quenching of [Ru^{II}(bpy)$_3$]$^{2+\star}$ by [Co^{III}(NH$_3$)$_5$Cl]$^{2+}$. The good agreement of the calculated and experimental results indicates that the oxygenation of NaSS occurs highly efficiently, once [Ru^{III}(bpy)$_3$]$^{3+}$ is formed by photoinduced electron transfer from [Ru^{II}(bpy)$_3$]$^{2+\star}$ to [Co^{III}(NH$_3$)$_5$Cl]$^{2+}$.

The dynamics of the photocatalytic oxidation of (TMPS)Mn^{III}(OH) with [Co^{III}(NH$_3$)$_5$Cl]$^{2+}$ in the presence of [Ru^{II}(bpy)$_3$]$^{2+}$ was also examined by laser flash photolysis measurements. Transient absorption spectra of (TMPS)Mn^{IV}(O) were obtained using a point-to-point technique, monitoring the change of absorbance after each laser pulse excitation ($\lambda = 450$ nm) of a phosphate buffer solution (pH 7.4) containing (TMPS)Mn^{III}(OH), [Ru^{II}(bpy)$_3$]$^{2+}$, [Co^{III}(NH$_3$)$_5$Cl]$^{2+}$, and NaSS at intervals of 5 nm (Fig. 3a; see also the transient absorption spectra of (TDCPS)Mn^{IV}(O) in Supplementary Fig. S3). The time interval between each laser pulse was 60 s, at which (TMPS)Mn^{III}(OH) is regenerated by the reaction of (TMPS)Mn^{IV}(O) with NaSS. In the absence of NaSS, (TMPS)Mn^{IV}(O) accumulates with each laser pulse. The transient absorption spectra in Fig. 3a agree with those of (TMPS)Mn^{IV}(O) obtained by the reactions of (TMPS)Mn^{III}(OH) with *m*-chloroperoxybenzoic acid (*m*-CPBA) (Fig. 3b)[28]. The Mn^{IV}(O) species is also produced by the thermal electron-transfer oxidation of (TMPS)Mn^{III}(OH) with 1 equiv. of [Ru^{III}(bpy)$_3$]$^{3+}$ in H$_2$O/CH$_3$CN (1:3, v/v) at 298 K, in which a new broad absorption band appears at 408 nm, accompanied by the disappearance of the absorption band at 467 nm due to (TMPS)Mn^{III}(OH) (Supplementary Fig. S4). The rates of oxidation of (TMPS)Mn^{III}(OH) and (TDCPS)Mn^{III}(OH) by [Ru^{III}(bpy)$_3$]$^{3+}$ were determined from the increase of the absorption band at 425 nm due to (TMPS)Mn^{IV}(O) and (TDCPS)Mn^{IV}(O), which obey pseudo-first-order kinetics. The observed pseudo-first-order rate constant increases linearly with concentration of (TMPS)Mn^{III}(OH) and (TDCPS)Mn^{III}(OH). From the slope of the linear plot, the second-order rate constants (k_{et}) of the oxidation of (TMPS)Mn^{III}(OH) and (TDCPS)Mn^{III}(OH) by [Ru^{III}(bpy)$_3$]$^{3+}$ were determined to be $4.1 \times 10^8\ M^{-1}\ s^{-1}$ and $4.1 \times 10^7\ M^{-1}\ s^{-1}$, respectively (Supplementary Fig. S5).

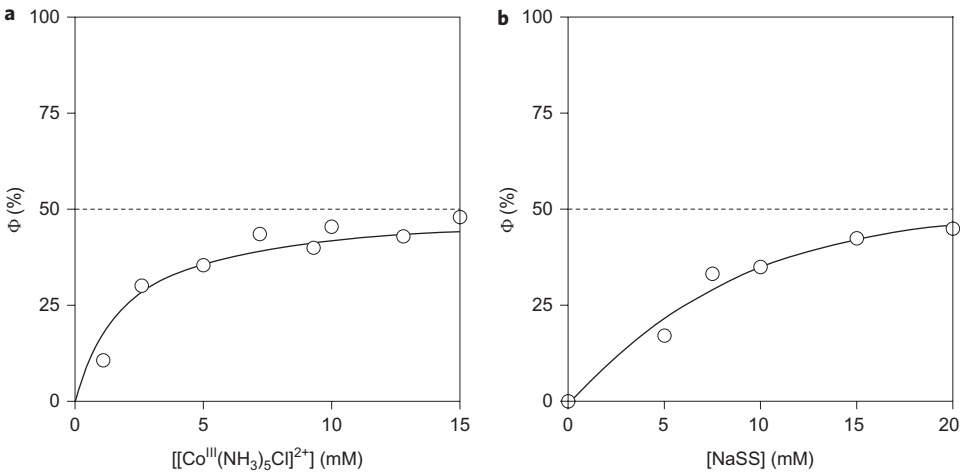

Figure 1 | Determination of quantum yields. a, Plot of quantum yield (Φ) versus [[Co^{III}(NH$_3$)$_5$Cl]$^{2+}$] obtained by photocatalytic oxygenation of NaSS (2.0×10^{-2} M) by [Co^{III}(NH$_3$)$_5$Cl]$^{2+}$, (TMPS)Mn^{III}(OH) (1.0×10^{-5} M) and [Ru^{II}(bpy)$_3$]$^{2+}$ (5.0×10^{-5} M) in a phosphate-buffered D$_2$O (pH 7.4). **b**, Plot of Φ versus [NaSS] obtained by photocatalytic oxygenation of NaSS by [Co^{III}(NH$_3$)$_5$Cl]$^{2+}$ (1.0×10^{-2} M), (TMPS)Mn^{III}(OH) (1.0×10^{-5} M) and [Ru^{II}(bpy)$_3$]$^{2+}$ (5.0×10^{-5} M) in a phosphate-buffered D$_2$O (pH 7.4).

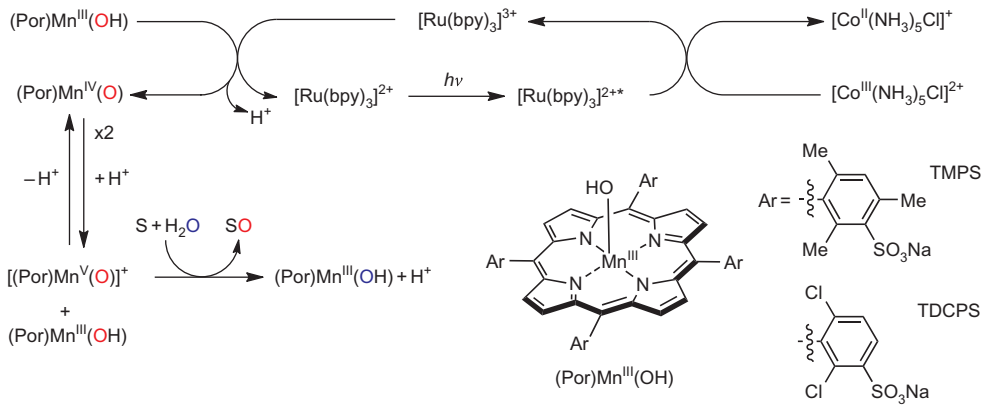

Figure 2 | Proposed reaction mechanism of photocatalytic oxygenations. (Por)Mn^{III}(OH) acts as an oxygenation catalyst and [Ru^{II}(bpy)$_3$]$^{2+}$ acts as a photocatalyst in the photocatalytic oxygenation of substrates. [(Por)Mn^{V}(O)]$^{+}$, produced by the disproportionation of (Por)Mn^{IV}(O), is the actual oxidant responsible for the oxidation of organic substrates.

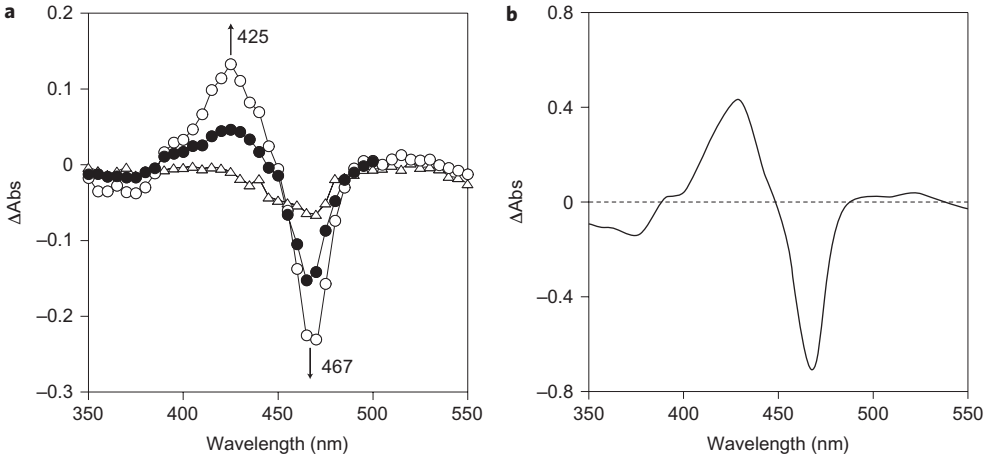

Figure 3 | Time-resolved absorption spectra of (TMPS)Mn^{III}(OH). a, Time-resolved absorption spectra observed at 0.016 ms (open triangles), 0.1 ms (filled circles) and 3.2 ms (open circles) after laser pulse excitation (450 nm) of a phosphate buffer solution (pH 7.4) containing (TMPS)Mn^{III}(OH) (7.0×10^{-6} M), [Ru^{II}(bpy)$_3$]$^{2+}$ (5.0×10^{-5} M), [Co^{III}(NH$_3$)$_5$Cl]$^{2+}$ (1.0×10^{-3} M) and NaSS (2.0×10^{-3} M). The transient spectra were obtained by a point-to-point technique, monitoring the change of absorbance after laser pulse excitation at intervals of 5 nm. The time interval between laser pulses was 60 s. **b**, Difference spectrum of (TMPS)Mn^{IV}(O) and (TMPS)Mn^{III}(OH). (TMPS)Mn^{IV}(O) was produced by the reaction of (TMPS)Mn^{III}(OH) (1.0×10^{-5} M) with 1.4 equiv. of *m*-CPBA in a borate buffer solution (pH 10).

As only (TMPS)Mn^{IV}(O) is produced by laser excitation and (TMPS)Mn^{IV}(O) reacts with NaSS thermally (Fig. 3a), [(TMPS)Mn^{V}(O)]$^{+}$ cannot be formed by the further oxidation of (TMPS)Mn^{IV}(O) with [Ru^{III}(bpy)$_3$]$^{3+}$ under the present experimental conditions. If such were the case, the maximum quantum yield of 50% (Fig. 1) would never be obtained.

The thermal reaction of (TMPS)Mn^{IV}(O) with NaSS was examined independently by monitoring the rise in the absorption band at 467 nm due to (TMPS)Mn^{III}(OH) after stopped-flow mixing of NaSS and (TMPS)Mn^{IV}(O); the latter was produced by the reaction of (TMPS)Mn^{III}(OH) (1.0×10^{-5} M) with 1.4 equiv. of *m*-CPBA in a phosphate buffer solution (pH 8.0). During the reaction, (TMPS)Mn^{IV}(O) was directly converted to (TMPS)Mn^{III}(OH) without any indication of the formation of (TMPS)Mn^{II}. The rate obeys second-order kinetics, even in the presence of a large excess of NaSS, and the second-order rate constant (k_{obs}) increases with increasing concentration of NaSS to reach a constant value (1.9×10^{3} M^{-1} s^{-1}) (Supplementary Fig. S6). In addition, the k_{obs} value increases linearly with proton concentration (Supplementary Fig. S7). These results suggest that the reaction of (TMPS)Mn^{IV}(O) with NaSS occurs via the disproportionation of (TMPS)Mn^{IV}(O) to give (TMPS)Mn^{III}(OH) and [(TMPS)Mn^{V}(O)]$^{+}$, the latter of which, as previously reported[21,29], is the actual oxidant for the oxygenation reactions.

The proposed photocatalytic mechanism is depicted in Fig. 2, where manganese porphyrins are denoted by (Por)Mn. The photocatalytic oxygenation of substrates (S) with H_2O begins by photoinduced electron transfer from [Ru^{II}(bpy)$_3$]$^{2+*}$ to [Co^{III}(NH$_3$)$_5$Cl]$^{2+}$ to produce [Ru^{III}(bpy)$_3$]$^{3+}$, which oxidizes (TMPS)Mn^{III}(OH) to (TMPS)Mn^{IV}(O). The latter intermediate disproportionates to produce [(TMPS)Mn^{V}(O)]$^{+}$ and (TMPS)Mn^{III}(OH). Substrates (S) are then oxygenated by [(TMPS)Mn^{V}(O)]$^{+}$ to yield oxygenated products (SO), accompanied by regeneration of (TMPS)Mn^{III}(OH) with H_2O. In this sequence, the oxygen atom in SO derives from H_2O, as demonstrated by ^{18}O-labelled water experiments (Supplementary Fig. S1). As photoinduced electron transfer from [Ru^{II}(bpy)$_3$]$^{2+*}$ to [Co^{III}(NH$_3$)$_5$Cl]$^{2+}$ occurs in an irreversible manner without involvement of back electron transfer[24,25], and the subsequent reactions occur thermally, all photons can be used to produce the oxygenated products with the maximum quantum yield of 50% (Fig. 1).

In conclusion, we have demonstrated here the development of photocatalytic electron-transfer oxygenation systems using water as an oxygen source. The manganese–oxo porphyrins are produced

by a weak one-electron oxidant $[Co^{III}(NH_3)_5Cl]^{2+}$ via photoinduced electron transfer, wherein the key step is an oxidative activation of water. Based on the kinetic studies, we have proposed that $[(Por)Mn^{V}(O)]^{+}$ is the active oxidant responsible for substrate oxygenation. The results reported herein open a new way to use water as an oxygen source for an oxygenation reaction using solar energy.

Methods

See the experimental section in the Supplementary Information for detailed experimental conditions and procedures, and spectroscopic and kinetic analyses.

Received 5 February 2010; accepted 12 October 2010; published online 28 November 2010

References

1. Lewis, N. S. & Nocera, D. G. Powering the planet: chemical challenges in solar energy utilization. *Proc. Natl Acad. Sci. USA* **103,** 15729–15735 (2006).
2. Yagi, M. & Kaneko, M. Molecular catalysts for water oxidation. *Chem. Rev.* **101,** 21–35 (2001).
3. Haumann, M. *et al.* Photosynthetic O_2 formation tracked by time-resolved X-ray experiments. *Science*, **310,** 1019–1021 (2005).
4. McEvoy, J. P. & Brudvig, G. W. Water-splitting chemistry of photosystem II. *Chem. Rev.* **106,** 4455–4483 (2006).
5. Yano, J. *et al.* Where water is oxidized to dioxygen: structure of the photosynthetic Mn_4Ca cluster. *Science* **314,** 821–825 (2006).
6. Barber, J. Photosynthetic energy conversion: natural and artificial. *Chem. Soc. Rev.* **38,** 185–196 (2009).
7. *Cytochrome P-450: Structure, Mechanism and Biochemistry* 3rd edn (Kluwer/Plenum, 2005).
8. Schlichting, I. *et al.* The catalytic pathway of cytochrome P450cam at atomic resolution. *Science* **287,** 1615–1622 (2000).
9. Dunford, H. B. & Stillman, J. S. On the function and mechanism of action of peroxidases. *Coord. Chem. Rev.* **19,** 187–251 (1976).
10. Pérez, U. & Dunford, H. B. Spectral studies on the oxidation of organic sulfides (thioanisoles) by horseradish peroxidase compounds I and II. *Biochim. Biophys. Acta* **1038,** 98–104 (1990).
11. Mlodnika, T. & James, B. R. *Metalloporphyrin Catalyzed Oxidations* (eds. Montanari, F. & Casella, L.) 121 (Kluwer, 1994).
12. Denisov, I. G. *et al.* Structure and chemistry of cytochrome P450. *Chem. Rev.* **105,** 2253–2277 (2005).
13. Meunier, B. Metalloporphyrins as versatile catalysts for oxidation reactions and oxidative DNA cleavage. *Chem. Rev.* **92,** 1411–1456 (1992).
14. Groves, J. T. *et al.* High-valent iron–porphyrin complexes related to peroxidase and cytochrome P-450. *J. Am. Chem. Soc.* **103,** 2884–2886 (1981).
15. Groves, J. T. & Watanabe, Y. Reactive iron porphyrin derivatives related to the catalytic cycles of cytochrome P-450 and peroxidase. Studies of the mechanism of oxygen activation. *J. Am. Chem. Soc.* **110,** 8443–8452 (1988).
16. Watanabe, Y. & Fujii, H. *Metal–Oxo and Metal–Peroxo Species in Catalytic Oxidations* (ed. Meunier, B.) 61 (Springer-Verlag, 2000).
17. Woo, L. K. *et al.* Thermodynamic and kinetic aspects of two- and three-electron redox processes mediated by nitrogen atom transfer. *J. Am. Chem. Soc.* **113,** 8478–8484 (1991).
18. Groves, J. T., Lee, J. & Marla, S. S. Detection and characterization of an oxomanganese(V) porphyrin complex by rapid-mixing stopped-flow spectrophotometry. *J. Am. Chem. Soc.* **119,** 6269–6273 (1997).
19. Nam, W. *et al.* Isolation of an oxomanganese(V) porphyrin intermediate in the reaction of a manganese(III) porphyrin complex and H_2O_2 in aqueous solution. *Chem. Eur. J.* **8,** 2067–2071 (2002).
20. Lane, B. S. & Burgess, K. Metal-catalyzed epoxidations of alkenes with hydrogen peroxide. *Chem. Rev.* **103,** 2457–2473 (2003).
21. Zhang, R., Horner, J. H. & Newcomb, M. Laser flash photolysis generation and kinetic studies of porphyrin–manganese–oxo intermediates. Rate constants for oxidations effected by porphyrin–Mn^{V}–oxo species and apparent disproportionation equilibrium constants for porphyrin–Mn^{IV}–oxo species. *J. Am. Chem. Soc.* **127,** 6573–6582 (2005).
22. Hirai, Y. *et al.* Ruthenium-catalyzed selective and efficient oxygenation of hydrocarbons with water as an oxygen source. *Angew. Chem. Int. Ed.* **47,** 5772–5776 (2008).
23. Lee, Y.-M. *et al.* Water as an oxygen source in the generation of mononuclear nonheme iron(IV) oxo complexes. *Angew. Chem. Int. Ed.* **48,** 1803–1806 (2009).
24. Low, D. W., Winkler, J. R. & Gray, H. B. Photoinduced oxidation of microperoxidase-8: generation of ferryl and cation-radical porphyrins. *J. Am. Chem. Soc.* **118,** 117–120 (1996).
25. Berglund, J. *et al.* Photoinduced oxidation of horseradish peroxidase. *J. Am. Chem. Soc.* **119,** 2464–2469 (1997).
26. Kanan, M. W. & Nocera, D. G. *In situ* formation of an oxygen-evolving catalyst in neutral water containing phosphate and Co^{2+}. *Science* **321,** 1072–1075 (2008).
27. Gafney, H. D. & Adamson, A. W. Excited state $Ru(bipyr)_3^{2+}$ as an electron-transfer reductant. *J. Am. Chem. Soc.* **94,** 8238–8239 (1972).
28. Arasasingham, R. D. & Bruice, T. C. The dynamics of the reactions of methyl diphenylhydroperoxyacetate with *meso*-tetrakis(2,6-dimethyl-3-sulfonatophenyl)-porphinatomanganese(III) hydrate and *meso*-tetrakis (2,6-dichloro-3-sulfonatophenyl)-porphinatomanganese(III) hydrate and imidazole complexes. Comparison of the reactions of manganese(III) and iron(III) porphyrins. *J. Am. Chem. Soc.* **113,** 6095–6103 (1991).
29. Fukuzumi, S. *et al.* Mechanistic insights into hydride-transfer and electron-transfer reactions by a manganese(IV)–oxo porphyrin complex. *J. Am. Chem. Soc.* **131,** 17127–17134 (2009).

Acknowledgements

This work was supported by a Grant-in-Aid (no. 20108010 to S.F.) and a Global COE program, 'the Global Education and Research Center for Bio-Environmental Chemistry' from the Ministry of Education, Culture, Sports, Science and Technology, Japan (to S.F.), and The National Research Foundation (NRF) and the Ministry of Education and Science Technology (MEST) of Korea through the WCU (R31-2008-000-10010-0) and GRL (2010-00353) Programs (to S.F. and W.N.) and the Creative Research Initiatives Program (to W.N.).

Author contributions

S.F., T.K. and W.N. conceived and designed the experiments. T.K. and H.K. performed the experiments. T.K. and H.K. analysed the data. Y.M.L. contributed materials/analysis tools. S.F. and W.N. co-wrote the paper.

Additional information

The authors declare no competing financial interests. Supplementary information accompanies this paper at www.nature.com/naturechemistry. Reprints and permission information is available online at http://npg.nature.com/reprintsandpermissions/. Correspondence and requests for materials should be addressed to S.F. and W.N.